Bull. Mater. Sci. (2021)44:186
https://doi.org/10.1007/s12034-021-02450-1

Investigation of novel diethanolamine dithiocarbamate agent for RAFT polymerization: DFT computational study of the oligomer molecules

ÜMİT YİLDİKO[1,*], AHMET ÇAĞRI ATA[2], ASLIHAN AYCAN TANRIVERDİ[2] and İSMAİL ÇAKMAK[2]

[1]Department of Bioengineering, Kafkas University, Kars 36100, Turkey
[2]Department of Chemistry, Kafkas University, Kars 36100, Turkey
*Author for correspondence (yildiko1@gmail.com)

MS received 2 December 2020; accepted 9 February 2021

Abstract. This study presents the successes in polystyrene (PS) synthesis through reversible additional fragmentation chain transfer (RAFT) polymerization. For RAFT polymerization of styrene, diethanolamine (DEA) RAFT agent was used. The PS synthesis has made significant progress in the control of the molecular weight distribution of polymeric products. The average molecular weight between 37113 and 43183 g mol^{-1} of PS determined by gel-permeation chromatography (GPC) was consistent with the accounted values. The controlled polymerization system also exhibited first-order linear kinetics and produced PS with slightly high dispersity (M_w/M_n = 1.42). The RAFT agents and polymers were characterized by NMR and Fourier transform-infrared (FTIR) spectroscopies, GPC), and differential scanning calorimetry (DSC). Besides, the structural and electronic properties for monomer, trimer and hexamer molecules on the DEA RAFT agent series were performed by density functional theory studies. Energy gap (Δ) values for monomer, trimer and hexamer were found to be 4.0396, 4.0943 and 4.0010 eV, respectively. These results show the chemical activity in the series and the charge transferability within the polymer. In the same series, the dipole moment values increased in parallel with the chain growth, as $\mu_{(D)}$ = 0.9124, 1.9951 and 2.0918, respectively.

Keywords. Controlled radical polymerization; RAFT; dithiocarbamate; DFT; diethanolamine.

1. Introduction

Polymers with well-defined architectures, predetermined molecular weights and narrow molecular weight distributions can be produced by the reversible addition-fragmentation chain transfer (RAFT) technique. Well-defined block [1] and graft copolymers [2], periodic or gradient copolymers [3], star and network structured functional end group polymers [4–6] and many other materials were obtained by a controlled radical mechanism. The controlled radical polymerization (CRP) technique [7,8] has some advantages in choosing monomers, functionality and purity of the polymer obtained, and even the price of the final product. In recent years, there are three effective CRP methods that can be applied to many monomers successfully; nitroxide-mediated radical polymerization (NMP) [9,10], atom transfer radical polymerization (ATRP) [11,12] and RAFT polymerization [13,14] method. The most important difference among these methods is the deactivators used. The deactivators used for NMP are nitroxides [15]. CRP methods are important methods used frequently in macromolecular engineering. In recent years, the RAFT polymerization has been widely used because it is applicable to a wide variety of monomers and reaction conditions (living polymerizations, both in solution and in aqueous dispersions [16,17]). Polymers that stabilize the RAFT polymerizations are used to mediate the formation of complex morphologies, to prepare multi-block polymers containing up to 20 blocks [18,19] and to prepare improved drug release to functionalize biomolecules with stabilizing polymers [19–23] in suspension polymerizations [19,24–27]. Besides, both polar and nonpolar monomers can be polymerized by this technique [17]. Xanthates and dithiocarbonyl compounds such as dithioester, tritiocarbonates, and some aromatic dithiocarbamates as a chain transfer agent are used in the RAFT methods [28,29]. Especially, it is used for free-radical polymerization of styrene, alkyl acrylates and vinyl acetate. By selecting an appropriate chain transfer agent, the synthesis of various polymers with predetermined molecular weight and low heterogeneity is possible [28]. Using the RAFT methodology, various polymers have been synthesized with controlled molecular weight and low dispersion, which have potential applications in different fields, such as biotechnology and leading-edge technologies of biomedical

Published online: 14 June 2021

and pharmaceuticals [30,31]. The RAFT methodology has become more practical due to research studies by scientists in the field of polymerization for different vinyl monomers [32].

Nowadays, the density functional theory (DFT) method has been widely used to provide information about the electronic and geometric structure of molecules [33]. The important feature of the polymer DFT is that the chain configuration, which is not taken into account in other DFTs, is an important issue informing the free energy function of the polymer DFT and in the proper relationship between the segment density profile and general potential [34]. With this method, structural properties of molecules, dipole moments, etc. can be calculated. In our literature search, we found that the theoretical DFT calculations of polymer compounds are in limited number. It is not possible to examine the huge size macromolecules with the level of technology available. However, it was aimed to predict the macromolecule size with the oligomer level study we applied here.

In our study, a novel dithiocarbamate-type DEA RAFT agent, which is one of the thiocarbonylthio compounds, was synthesized and analysed by known spectroscopic methods. The DEA RAFT agent was used in the controlled radical polymerization of styrene. The DFT/B3LYP method with 6-311G (d, p) basis set was used in the computing of optimization and the highest occupied molecular orbital (HOMO)–lowest unoccupied molecular orbital (LUMO) energy gaps of the selected oligomeric polystyrene (PS)-RAFT agents. The results were interpreted by the small molecule approach method for the polymer through monomer, trimer and hexamer structures.

2. Materials and methods

2.1 *Materials*

Diethanolamine (≥98.0%), carbon disulphide (99%), potassium hydroxide (85%), benzoyl chloride (99%), *N,N*-dimethylformamide (99%) and benzene were commercially obtained from Sigma-Aldrich or Merck. Styrene and 2,2′-azobisisobutyronitrile (AIBN) 99% was crystallized from toluene. Sodium sulphate (99.5%) and methanol (99%) were purchased from the Emboy product.

2.2 *Instrumentation*

Gel-permeation chromatography (GPC) chromatograms were obtained using a Waters 510 instrument using tetrahydrofuran as the solvent at a flow rate of 1 ml min^{-1}, with a Waters 1515 isocratic HPLC pump equipped with a Waters 2414 refractive index detector and three Waters Styragel HR columns. Gel-permeation chromatography (GPC) chromatograms were obtained using a Waters 510 instrument using tetrahydrofuran as the solvent at a flow rate of 1 ml min^{-1}. With Waters 1515 isocratic HPLC pump equipped with Waters 2414 refractive index detector and three Waters styragel HR columns that a calibration curve was generated six of low dispersity purchased from Polyscience. BUCHI R-200 Model device was used to evaporate the solvent from the solutions. NMR spectra were recorded at 400 MHz (^{1}H) and 151 MHz (^{13}C) at 298 K using tetramethylsilane (0 ppm) as the internal reference. NMR spectroscopic data were recorded in $CDCl_3$ using as internal standards, the residual non-deuterated signal for ^{1}H NMR and the deuterated solvent signal for ^{13}C NMR spectroscopy. DSC-60 SHIMADZU with 10°C min^{-1} heating rate under nitrogen gas 100 ml min^{-1} was used to determine the glass transition temperatures and melting temperatures of the polymers.

2.3 *Experimental procedure*

2.3a *Preparation of the dithiocarbamate DEA RAFT agent:* Solid sodium hydroxide (5.62 g, 0.1 mol) was added to a solution of diethanolamine (10.5 ml, 0.108 mol) in *N,N*-dimethylformamide (DMF) in one portion at room temperature under N_2 atm. and the resulting mixture was stirred for 3 h. Then carbon disulphide (6.25 ml, 0.1 mol) was added dropwise to the reaction mixture. The resulting reaction mixture was heated for 18 h at reflux temperature. Benzoyl chloride (11.6 ml, 0.1 mol) was added and stirred in a water-ice bath to remove the exothermic heat of the mixture (obtained a light orange-yellow colour). The obtained solution was stirred for 1 day and then filtered through a filter paper to the flask. The solvent (DMF 153°C) in the flask was evaporated at 60°C in a vacuum evaporator. DMF in the solvent was evaporated for a total of 25 h due to its low volatility. The solution was precipitated in diethyl ether and allowed to stand in the refrigerator for 24 h. After 1 day, the solution portion was decanted and left in the fume cupboard. The reaction of synthesis is shown in scheme 1. After 24 h, the solution portion was placed in the vacuum oven to ensure complete drying. It was observed that the weighing was fixed after 14 h. As a result of weighing, 24.18 g RAFT agent was obtained in 78% yield. Fourier transform-infrared (ν, cm^{-1}): 3307, 2954, 2884, 2784, 2505, 2361, 1720, 1649, 1597, 1444, 1408, 1271, 1060, 1028, 937, 867, 786, 716, 544 (supplementary figure S1). ^{1}H NMR (400 MHz, $CDCl_3$, δ, ppm): 8.14 (2H, d, aromatic), 7.82 (1H, s, aromatic),7.52 (2H, d, aromatic), 5.15 (2H, bs, O*H*–CH_2), 3.81(H, d, OH–C*H*$_2$–CH_2–), 3.13(H, d, OH–CH_2–C*H*$_2$–), ^{13}C NMR (100 MHz, $CDCl_3$ δ, ppm): 171.5, 166.0, 163.8, 137.7, 133.9, 130.1, 129.72, 129.68, 129.3, 129.1, 128.9, 128.6, 127.2, 58.9, 58.8, 56.9, 56.7, 50.4, 49.5, 45.0, 40.3, 40.2, 40.1, 39.9, 39.6, 39.5.

2.3b *Polymerization of styrene via dithiocarbamate RAFT agent:* The components of styrene polymerization are as

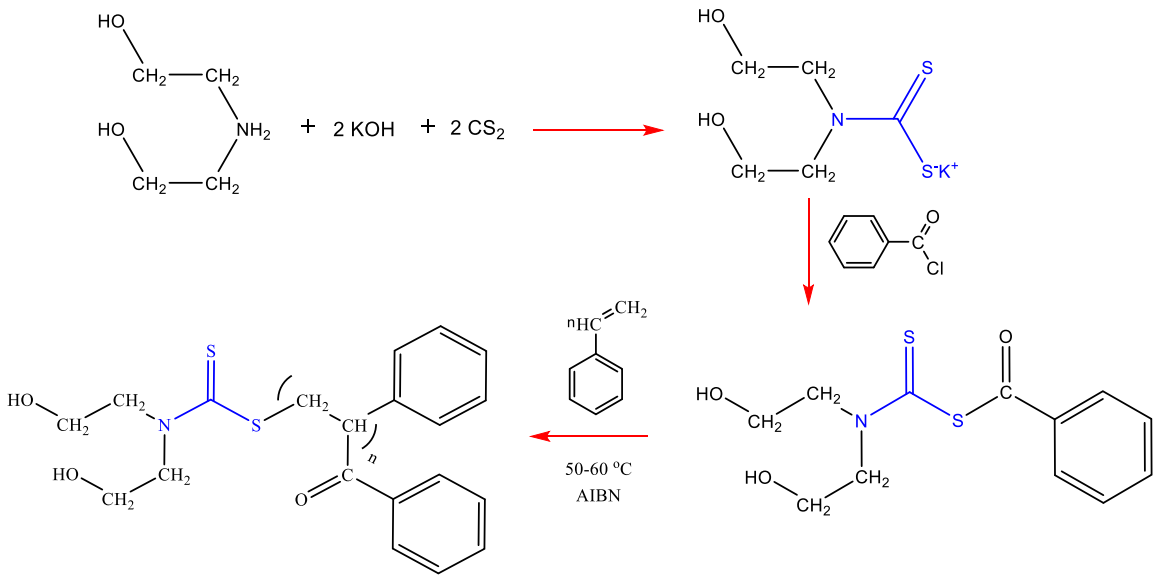

Scheme 1. Synthesis of DEA RAFT agent and controlled polymerization of styrene.

follows: $[\text{styrene}]_0/[\text{RAFT agent}]_0/[\text{AIBN}]_0$ = 1000:8:1.6 M ratios. Dimethylformamide (10 ml) was added over styrene (10 ml, 0.0874 mol). CTA (0.2 g, M_w = 256 g mol^{-1}) was added to the resulting mixture and stirred until dissolved. Then, 2,2′-azobis(isobutyronitrile) (AIBN; 0.0234 g, 0.14 mmol) was added to the reaction mixture as an initiator. The mixture was distributed into ten tubes with a magnetic stirrer bar. The reaction mixture was left in the ultrasonic bath for about 10 min and purged with argon gas for a further 3 min. Polymerization was initiated at 60–65°C for desired time. The polymerization reactions were terminated sequentially and precipitated in methanol at 24 h periodic intervals (scheme 1). The polymers were dried in a vacuum oven at 200-bar pressure at 45°C and waited until fixed weighing was reached. Fourier transform-infrared (ν, cm^{-1}): 3103, 3058, 3024, 2969, 2920, 2848, 2360, 2338, 1740, 1661, 1640, 1600, 1491, 1448, 1368, 1215, 1066, 1027, 906, 842, 751, 695, 537 (supplementary figure S2). ^{1}H NMR (400 MHz, $CDCl_3$, δ, ppm): 8.14 (2H, d, aromatic), 7.82 (1H, s, aromatic), 7.52 (2H, d, aromatic), 8.14 (4H, q aromatic), 7.82 (1H, s, aromatic), 5.31 (H, d, CH_2=CH–) 5.15 (2H, bs, OH–CH_2), 3.81 (H, d, OH–CH_2–CH_2–), 3.13 (H, d, OH–CH_2–CH_2–).

3. Results and discussion

3.1 *DEA dithiocarbamate RAFT agent synthesis and usage in styrene polymerization*

In the RAFT polymerization technique, the combination of the monomer and the RAFT agent used is an important factor in the success of the RAFT agent. The efficiency of this RAFT agent is largely determined by the correct selection of R and Z groups in the design of the RAFT agent. In the structure design of the RAFT agent, diethanolamine compound was used as the Z group [35]. The compound that provides reversible chain transfer and controlled growth is dithiocarbamate-type RAFT agent [19]. In the presence of the AIBN initiator, the most common azo initiator, the styrene was polymerized using the DEA RAFT agent [36]. The polystyrene (PS), containing end functional –OH groups, was synthesized with RAFT agent. GPC analysis of molecular weight values of synthesized polymers was performed.

In$[M]_0/[M]$–polydispersity index (PDI)–time and M_{nGPC}–M_{nTeo}–time graphs plotted according to the results obtained from GPC analysis for all polymerization data are shown in figures 1 and 2 and table 1 [37]. GPC results of the PSs are given in figure 3. The molecular weight control of RAFT polymerization can be understood from the data obtained by

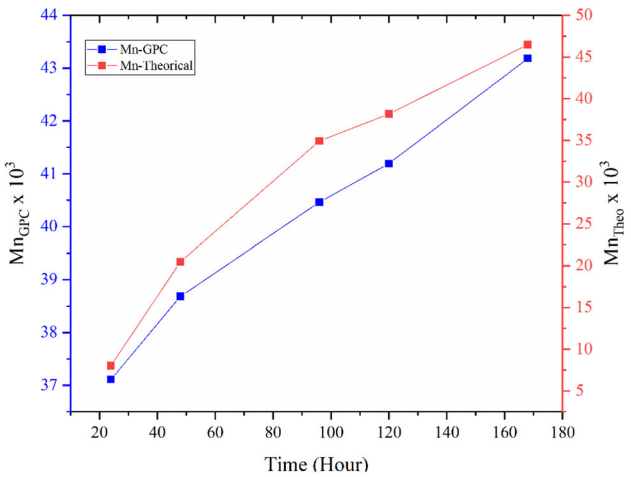

Figure 1. Mn_{GPC}–Mn_{Theo}–time graph of styrene polymerization with DEA RAFT agent.

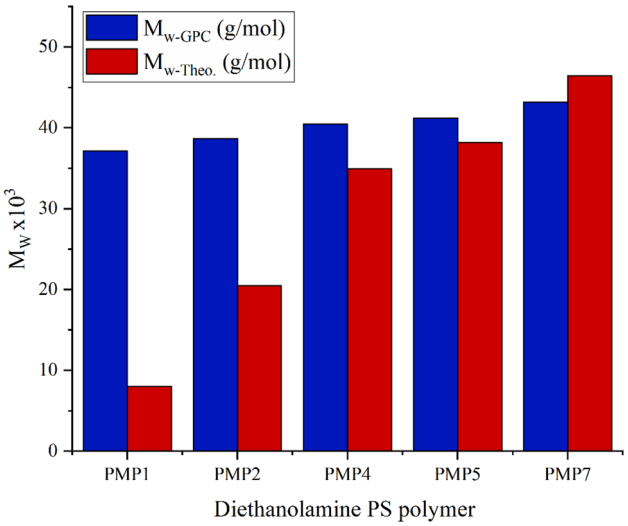

Figure 2. The comparison chart of molecular weight–PS with RAFT agent.

the linear increase of the Mn–time plot. The linear kinetic plot of $\ln([M]_0/[M])$ *vs.* polymerization time showed that polymerization was first order with reference to the monomer concentration. The kinetic rate constant is calculated as $k = 2.09 \times 10^{-6}$ min^{-1}. During polymerization, their molecular weights increase in direct proportion to the monomer consumption. Also, polydispersity is expected to have constant values as a result of the control of RAFT polymerization [38]. According to figure 4, the polymer has approximately the same PDI values during the reaction. This result showed that the molecular weight distribution of polymers obtained by control RAFT polymerizations is quite narrow. Considering that the PDI value of the monodisperse distribution is 1, the values of RAFT ranging from 1.42 to 1.44 are quite consistent [39,40]. All these indicate that RAFT polymerization of PS was controlled.

Polystyrene with narrow molecular weight distribution is obtained by dithiocarbamate DEA RAFT agent. RAFT agent; was characterized by Fourier transform-infrared, ^{1}H NMR and ^{13}CNMR spectroscopy, while PS was also characterized by GPC (supplementary figures S3, S4 and S5) and differential scanning calorimetry (DSC) analyses.

The ^{1}H NMR spectra of RAFT agent shown in figure 5 have $–CH_2$ protons at 1–2 ppm, $–CH_3$ protons bound to the benzene ring at 2.5 ppm, –CH protons at 3.6–5 ppm, and –CH protons on the aromatic structure are seen to be at 7.5–8 ppm. The ^{1}H NMR spectra of the block copolymer shown in figure 6 are examined, $–CH_2$ protons bound to nitrogen in DEA structure at 2.9–3 ppm, the protons of the –OH group at 3.5–3.8 ppm, $–CH_2$ protons bound to the –OH group at 3–3.5 ppm and –CH protons on the aromatic structure are seen to be at 6.5–8 ppm. The ^{13}C NMR spectra of the dithiocarbamate DEA RAFT agent in figure 7, have the solvent at 40 ppm, $–CH_2$ protons attached to the –OH group at 50 ppm, $–CH_2$ protons attached to nitrogen groups at 58 ppm, and –CH groups on the aromatic ring are seen to illuminate at 130 ppm. The DSC shown in figure 8 is examined, phase transitions are seen and the T_g value of the polymer was calculated as 34°C. In Fourier transform-infrared spectroscopy, alcohol peak at 3281.70 cm^{-1} indicates alcohol at the two ends of DEA. Another peak is the secondary amine peak of the secondary order amine at 3310–3350 cm^{-1}. This is because it is in the same range as the severe alcohol peak and overlaps with the amine peak. In Fourier transform-infrared spectrum of the DEA (supplementary figure S6), the peak is between 3000 and 3100 cm^{-1}, just above the value of peak 3000 cm^{-1} in the spectrum show us that either the alkene or aromatic structure enters the molecule. The overtones seen at 2000 cm^{-1} give us the exact result of the aromatic ring entering the structure. The characteristic carbonyl peak seen at 1720.38 cm^{-1} indicates that the reaction was carried out in the desired manner. In the IR spectrum of the RAFT agent, the strong peak of C=S bond was observed at 1050 cm^{-1} and the strong peak C–S bond 698 cm^{-1} was observed.

3.2 *Polymerization mechanism of DEA RAFT*

3.2a *Initiation:* The active centre with the cyanopropyl radical was created by thermally degrading (60°C) of the

Table 1. PS characteristics obtained for radical polymerization of styrene with dithiocarbamate RAFT agent.

Experiment no.	Experiment code[a]	Time (h)	Substance amount[e]	$\ln[M]_0/[M]$	[b]M_{Theo} (g mol^{-1})	[c]M_{GPC} (g mol^{-1})	[d]D (M_w/M_n)	Efficiency, %
1	PMP_1	24	0.2475	0.3178	8014	37,113	1.44	27.23
2	PMP_2	48	0.4005	0.5808	20,485	38,687	1.42	44.06
3	PMP_4	96	0.5273	0.8677	34,922	40,462	1.42	58.01
4	PMP_5	120	0.5510	0.9318	38,187	41,193	1.42	60.62
5	PMP_7	168	0.6143	1.1264	46,462	43,183	1.42	67.58

[a]Each polymerization was performed in *N,N* dimethylformamide using RAFT agent.
[b]$M_{n,theo}$ = [styrene]/[RAFT agent] × M_w (styrene) × conv.) + M_w (RAFT agent).
[c,d]Determined by means of GPC in tetrahydrofuran eluent using polystyrene standards.
[e]Calculated by gravimetric results.

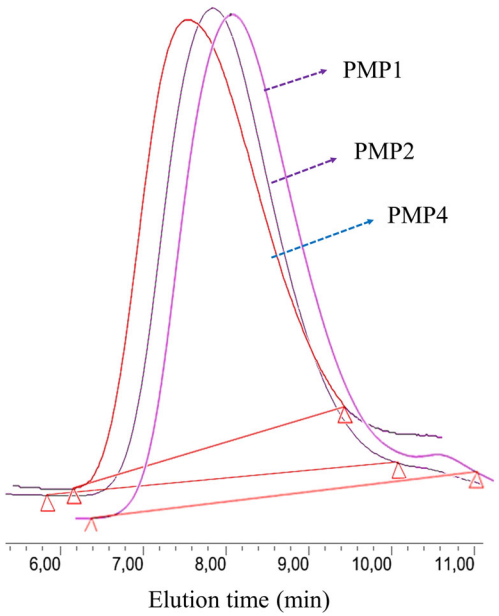

Figure 3. GPC chromatography of PS polymer with DEA RAFT agent.

azobisisobutyronitrile compound from the radical initiator. The radical end obtained in the starting step will remain active by adding styrene throughout the entire reaction. The radical source of the reaction was formed at this step. Adding styrene, an important member of the vinyl monomer group, a polymer chain with a $PS^{\bullet}$ radical tip is formed, as shown in scheme 2.

3.2b *Pre-equilibrium:* These chemicals, known as RAFT agents or chain transfer agents, are thiocarbonylthio compounds and have two different functional groups in their structure. These two functional groups Z and –R have different functions. The function of the –Z group is to provide that radical groups are easily attached to the thiocarbonyl (C=S) bond, where the compound used as the Z group is the $–NR_2$ group. The dietethanol group was used as the Z group. The R group –benzoyl separates to form a radical end. In the first step of the polymerization, by adding thiocarbonylthio [RSC(Z) = S'(1)] growing radical and following processes, intermediate product radical $R^{\bullet}$ and a polymeric dithiocarbamate compound are formed.

3.2c *Propagation:* The cleavage group ($–R^{\bullet}$) that is released at the end of the reaction reacts with one of the styrene monomers in the medium to form a separate active polymer chain. The active chain obtained in this step will be exposed to growth-fragmentation and balancing steps on its own. In this case, ($R\text{-}PS^{\bullet}$) occurs by a new radical ($R^{\bullet}$) and monomer addition reaction.

3.2d *Core-equilibrium:* The capture of the growing active macro RAFT agent by the radical group and the $R\text{-}PS^{\bullet}$ thiocarbonyl compounds constitute the most basic

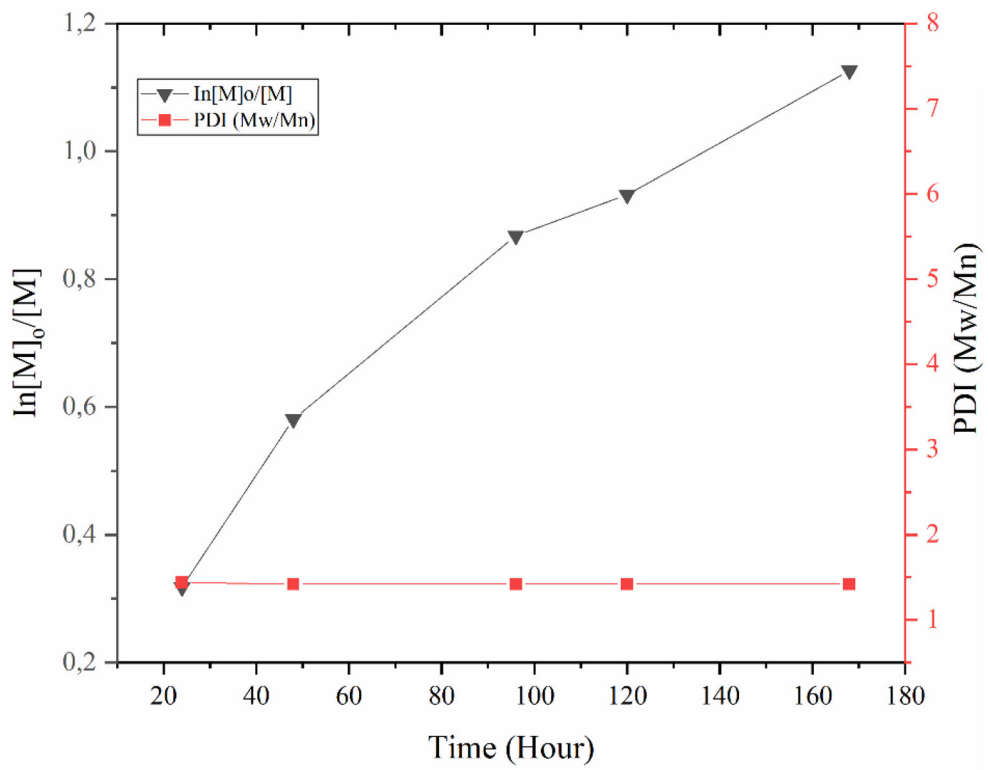

Figure 4. In$[M]_0/[M]$–PDI–time graph of styrene polymerization with DEA RAFT agent.

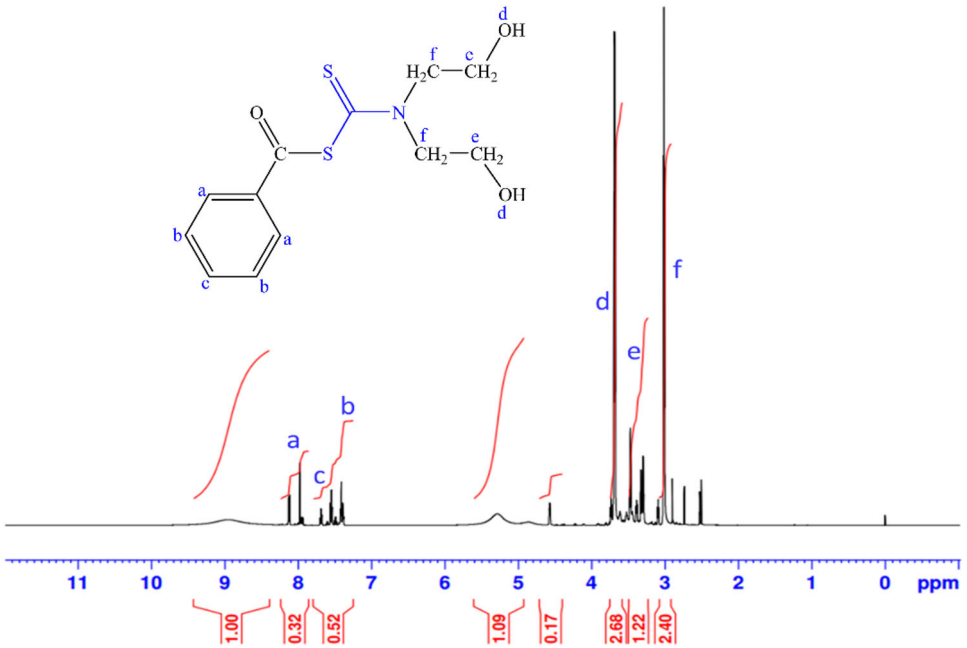

Figure 5. ^{1}H NMR spectrum of DEA RAFT agent.

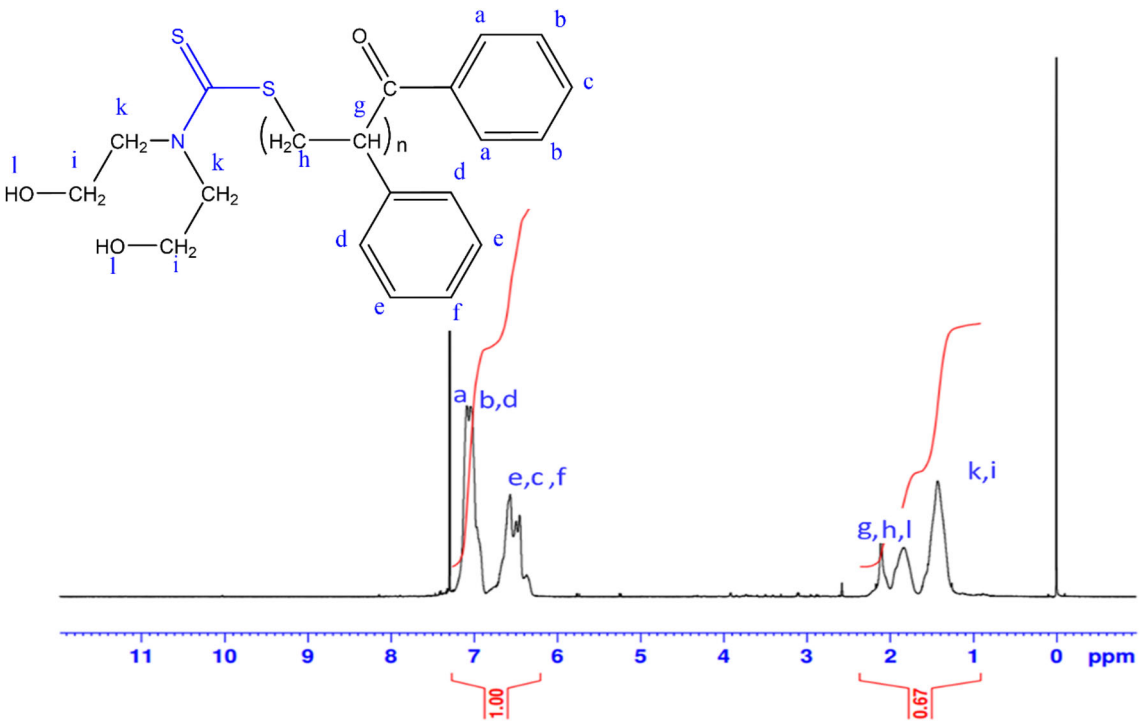

Figure 6. ^{1}H NMR spectrum of PS with DEA RAFT agent.

step of polymerization that is balancing by the reversible reaction. Thus, the chain termination step seen in conventional radical polymerization is not seen in this system. With the radical group of active growing macro RAFT agent and R-PS$^{\bullet}$, by rapid balance and the effect of dominant polymeric thiocarbonylthio compounds allow equal growth for all chains and enable the production of polymers with narrow molecular weight distribution.

3.2e *Termination:* There is no termination in RAFT, but there is termination with external influence. The termination step of RAFT polymerization is suppressed by the reduction of the radical concentration. The termination is

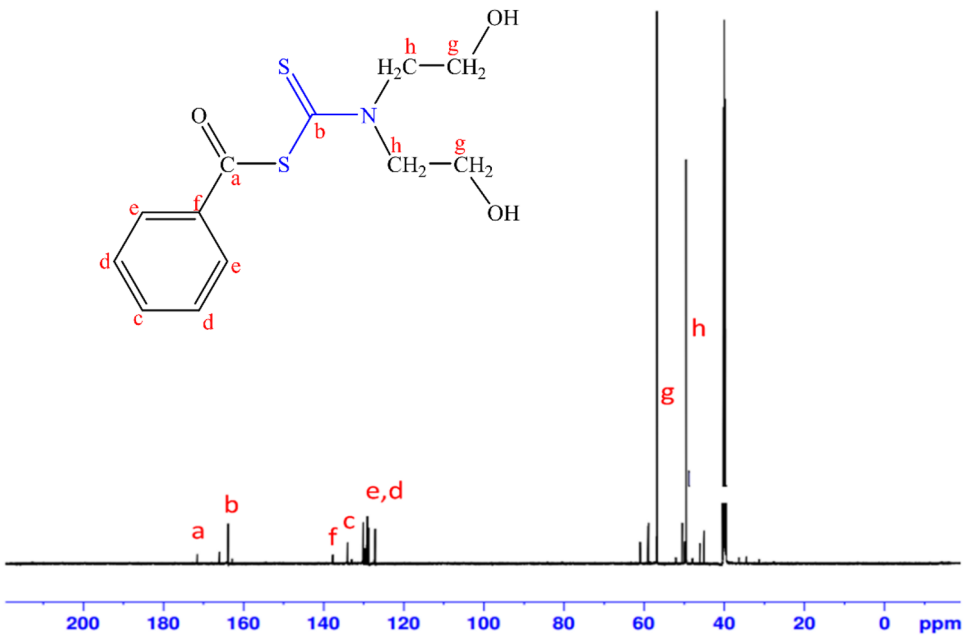

Figure 7. ^{13}C NMR spectrum of DEA RAFT agent.

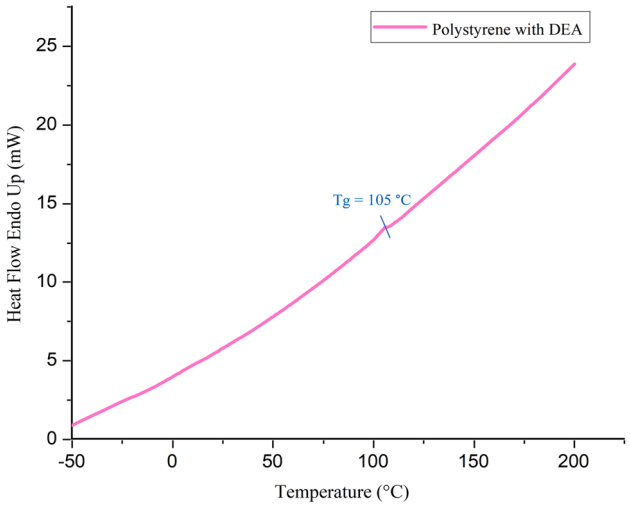

Figure 8. DSC analysis of the polystyrene with DEA RAFT agent.

accomplished by manually stopping the reaction mixture. Thus, a styrene monomer is removed from the actively growing chains and PS-polymer is obtained at the termination step [41,42].

3.3 *DFT studies of oligomer styrene with dithiocarbamate DEA RAFT agent*

DFT, besides being an important approach to atomic and molecular electronic structure, is used for calculations based on quantum mechanics principles at the atomic level. Besides, it is reliable in meeting the need for self-interaction of ionizations and atomizations occurring, providing qualitatively correct electronic structures. It also allows more reliable evaluation in the calculation of magnetic anisotropies, inter-ion exchange parameters, and spin excitations. For this reason, it was inevitable to choose and use the DFT method [43–46]. The DFT method is used to calculate monomers, oligomers and polymers. According to their different formulations and applications, DFT can be classified as atomic DFTs, molecular DFTs and polymer DFTs. A multidimensional DFT and a 3-D molecular DFT were developed to estimate the unsolvated energy of small organic molecules, respectively [34,47].

3.3a *Geometry optimization:* DFT studies, Becke, three-parameter, Lee-Yang-Parr (B3LYP) method with 6-311G (d, p) basis set in Gaussian 09 program were used [48]. Optimized ground-state structure and total energy conversion of monomer, trimer and hexamer depending on the RAFT agent in controlled styrene polymerization are given in figure 9. The optimized bond length parameters of PS with the end of RAFT molecule calculated with B3LPY/6-311G (d, p) level are listed in table 2. A comparison was made by giving all the values calculated from the optimized geometry of monomer, trimer and hexamer. The optimization means that the structure has minimum potential energy [49,50].

The bond distances of the thiocarbonylthio compound were found for the sulphur compounds, for monomer 1.712–1.903 Å, for trimer 1.716–1.902 Å and for hexamer 1.716–1.903 Å, respectively. All bond lengths and bond angles in the phenyl rings are in the same range. C–C bond distances are in the range of 1.403–1.408 Å for monomer, trimer and hexamer, while for C–N these values are in the range of 1.357–1.481 Å and belong to the nitrogen atom in

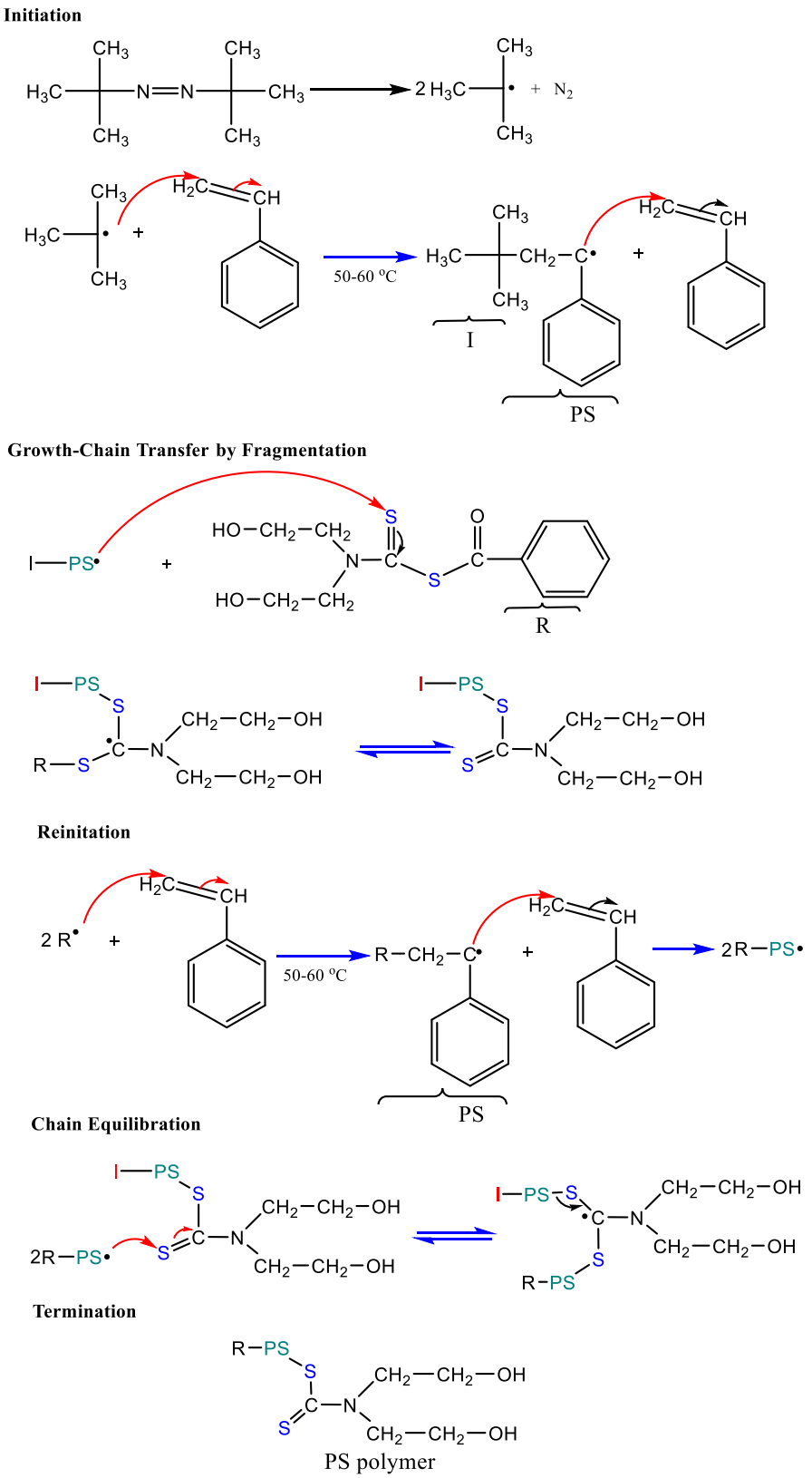

Scheme 2. The RAFT polymerization mechanism of styrene with DEA RAFT agent.

the aliphatic group. C–H bond lengths are in the range of 1.078–1.079 Å for monomer, trimer and hexamer in bond distances of the aromatic ring, C–H bond lengths are in the range of 1.088–1.089 Å in the aliphatic group and bond

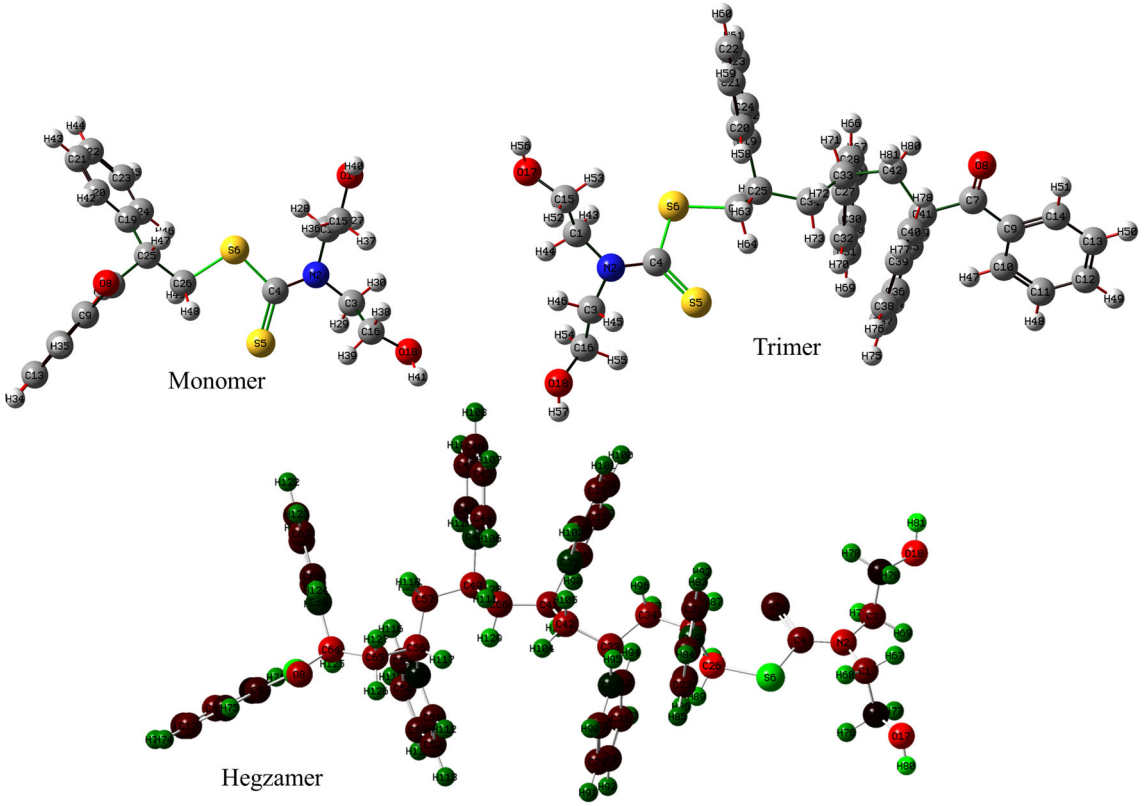

Figure 9. The optimized structure of the compound using B3LPY/6-311G (d,p) basis set.

lengths lie in the range of 1.248–1.457 Å in C–O region. C–C–C angles are between 120° and 120.5°, C–N–C angles are between 119° and 124°, S–C–S angles are between 121° and 122°, and finally, C–C–O angles are between 104° and 122° for monomer, trimer and hexamer compounds. As seen in table 2, although the molecular structures of the

Table 2. Theoretically obtained bond lengths (Å) and bond angles (°) of the monomer, trimer and hexamer.

	Bond lengths (Å)				Bond angles (°)		
Atom groups	Monomer	Trimer	Hexamer	Atom groups	Monomer	Trimer	Hexamer
C1–N2	1.482	1.481	1.481	C1–N2–C3	116.66	115.07	114.99
C3–N2	1.484	1.481	1.481	C1–N2–C4	123.32	124.08	124.20
C4–N2	1.357	1.355	1.355	C3–N2–C4	119.95	120.84	120.80
C1–C15	1.527	1.527	1.527	N2–C4–S5	124.93	124.28	124.27
C3–C16	1.527	1.525	1.525	N2–C4–S6	113.56	113.22	113.28
C15–O17	1.455	1.456	1.455	C1–C15–O17	104.55	104.85	104.92
C4–S5	1.712	1.716	1.716	C3–C16–O18	104.68	105.05	105.06
C4–S6	1.862	1.862	1.861	C25–C26–S6	108.68	112.98	113.38
C16–O18	1.457	1.456	1.457	C9–C10–C11	120.37	120.45	120.45
C26–S6	1.903	1.902	1.903	C20–C21–C22	120.15	120.08	120.08
C7–O8	1.248	1.249	1.249	S5–C4–S6	121.49	122.48	122.43
C9–C14	1.408	1.407	1.407	O8–C7–C9	120.08	119.77	119.77
C19–C24	1.401	1.403	1.403	C7–C9–C10	123.58	123.49	123.43
C1–H28	1.087	1.088	1.088	C1–N2–C3–C16	99.476	93.156	–93.11
C3–H30	1.087	1.088	1.088	C1–N2–C4–S5	179.02	179.15	179.12
017–H40	0.971	0.971	0.971	C1–N2–C4–S6	–0.021	0.926	1.310
O18–H41	0.971	0.971	0.971	N2–C1–C15–O17	178.13	173.07	173.07
C10–H31	1.078	1.079	1.079	C9–C10–C11–C12	0.172	0.013	0.065

monomer, trimer and hexamer compounds have grown, there are very small differences between their values.

3.3b *HOMO and LUMO analysis:* The main electronic parameters related to orbitals in a molecule are the highest occupied molecular orbital (HOMO) and the lowest unoccupied molecular orbital (LUMO) and occur in their energy gap. HOMO is the outermost (highest energy) orbital electron that can function as an electron donor. LUMO is the innermost (lowest energy) orbital that has adequate space to accept electrons and can act as an electron acceptor [51,52]. The volume orbital of HOMO and LUMO for BAPMB is shown in figure 10. In addition, $LUMO_{+1}$ and $HOMO_{-1}$ graphics of the compound are taken. From figure 10, HOMO –6.08 eV and LUMO –2.04 eV value for the monomer, HOMO –5.97 eV and LUMO –1.88 eV value for trimer and HOMO –5.89 eV and LUMO –1.89 eV value for hexamer belonging to the molecule was calculated. For other orbitals; $HOMO_{-1}$ –6.38 eV and $LUMO_{+1}$ –1.19 eV value for monomer, $HOMO_{-1}$ –6.21 eV and $LUMO_{+1}$ –1.03 eV value for trimer and $HOMO_{-1}$ –6.12 eV and $LUMO_{+1}$ –0.95 eV value for hexamer were calculated. The HOMO and LUMO orbitals determine how the molecule interacts with other species. In the same way, the bandgap helps to characterize their chemical reactivity and their kinetic stability. It also demonstrates polarization, hardness, electronegativity, and other reactive indexes of a molecule with a small border orbital space [53–57]. Table 3 shows the chemical reactivity indexes.

The bandgap values were evaluated with a new approach and this value turned out to be 4.0 eV. Of course, the expected value cannot be achieved in macromolecules with a high number of atoms. However, it is possible to make evaluations of molecules with 300–400 atoms. The electrical properties of materials are closely related to the electronic band structure. If the energy bands are completely filled or completely empty, the crystal acts as an insulator because electrons cannot move (they cannot carry charges) because there are no empty places in the band when the electric field is applied (E_{gap} insulator (5.4 eV) >> E_{gap} semiconductor (0.6 eV)) [58]. Our result is close to the insulator. Semiconductor values are lower than the result we got. The values may not exactly reflect the polymer, but the electrical properties of the material have been tried to be elucidated with the small molecule group approach. It is known in the literature that this approach is used [59,60].

Optimized bond angles of the compound selected on the basis of B3LYP/6-311G (d, p) of monomer, trimer and hexamer are shown table 3. The difference between them is very small and this difference is a good match between the oligomer systems.

3.3c *Mulliken population analysis:* The calculating Mulliken atomic charges have an important role in the

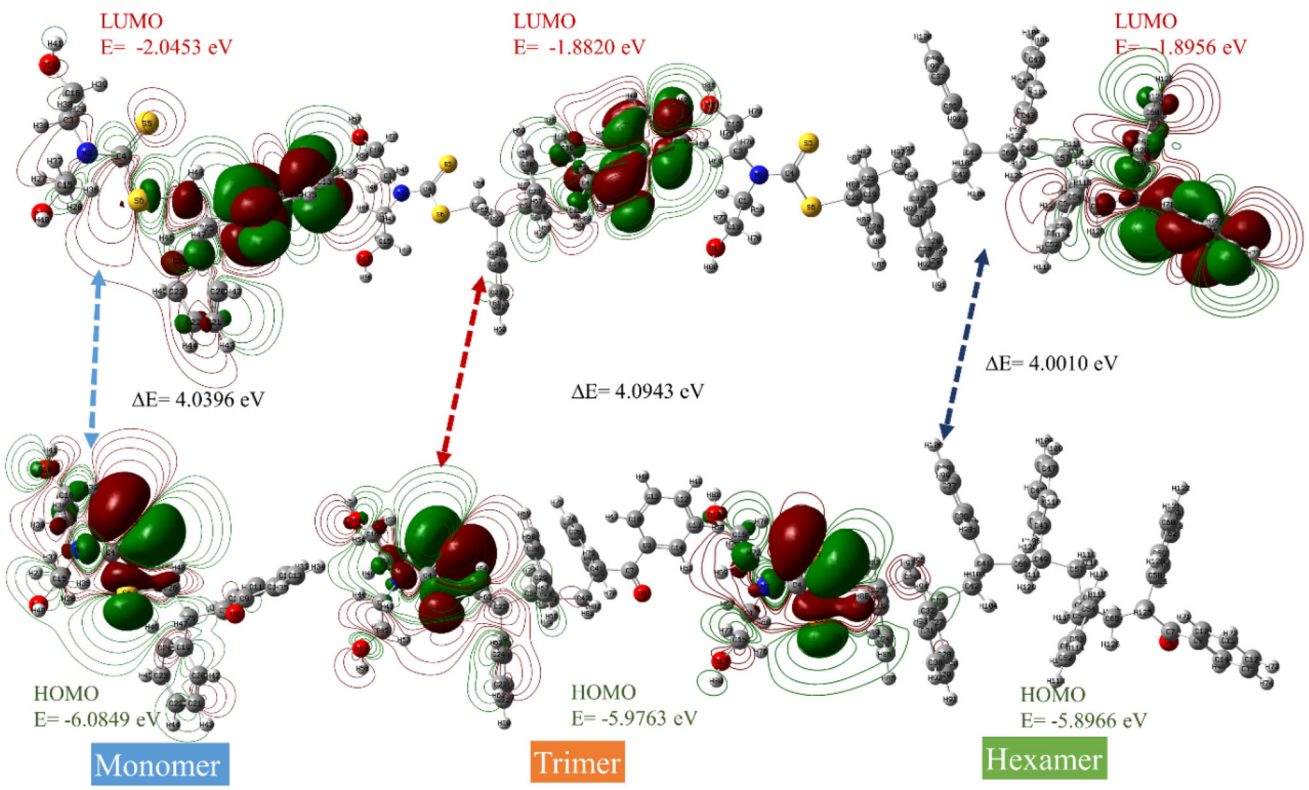

Figure 10. Frontier orbitals composition of agent monomer, trimer and hexamer molecules with DEA RAFT agent.

Table 3. Comparison of HOMO, LUMO, energy gaps, etc., and properties of related monomer, trimer and hexamer.

Molecular parameters	Monomer	Trimer	Hexamer
E_{HOMO} (eV)	−6.0849	−5.9763	−5.8966
E_{LUMO} (eV)	−2.0453	−1.8820	−1.8956
E_{HOMO-1}	−6.3818	−6.2101	−6.1260
E_{LUMO+1}	−1.1902	−1.0327	−0.9532
Energy gap (Δ) $\lvert E_{HOMO}–E_{LUMO}\rvert$	4.0396	4.0943	4.0010
Ionization potential ($I = -E_{HOMO}$)	6.0849	5.9763	5.8966
Electron Affinity ($A = -E_{LUMO}$)	2.0453	1.8820	1.8956
Electronegativity ($\chi = (I+A)/2$)	4.0651	3.9292	3.8961
Chemical potential ($\mu = -(I+A)/2$)	−4.0651	−3.9292	−3.8961
Chemical hardness ($\eta = (I - A)/2$)	2.0198	2.0472	2.0005
Chemical softness ($s = 1/2\eta$)	1.0099	1.0238	1.0003
Electrophilicity index ($\omega = \mu^2/2\eta$)	4.0907	3.7707	3.7939

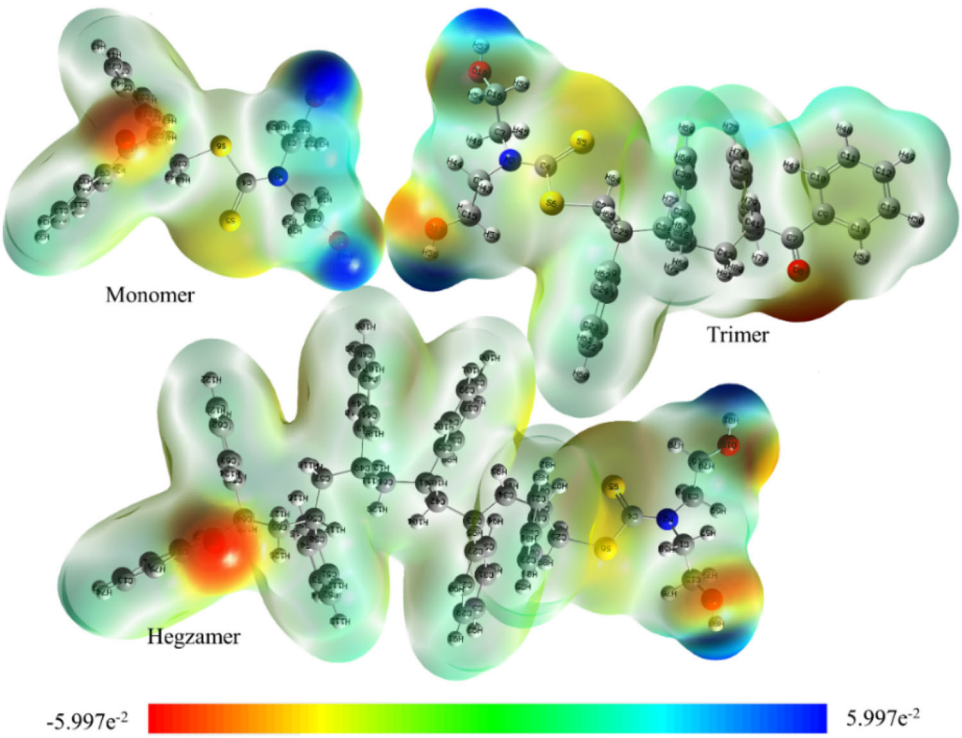

Figure 11. MEP of polystyrene with RAFT agent.

application of quantum chemical calculation on the molecular system [61,62], because atomic charges affect the dipole moment, molecular polarization, electronic structure, and many properties of molecular systems. The charge distribution on the atom shows the formation of the donor and acceptor pair, including the charge transfer in the molecule [63]. The Mulliken charge atom was calculated on the B3LYP/6-311G basis set of monomer, trimer and hexamer. Mulliken charge distribution for sulphur (S) atoms; monomer (0.056), trimer (–0.058) and hexamer (–0.059), monomer (0.477), trimer (0.414) and hexamer (0.411), and then for oxygen (O) atom; monomer O8-017-O18 (−0.316)-(−0.616)-(0.619), trimer O8-017-O18 (−0.308)-(−0.601)-(−0.600) and hexamer O8-017-O18 (−0.311)-(−0.602)-(−0.601) were found, respectively. The charge value of the C atom in the PS has a positive charge for C41 atom; monomer (0.816), trimer (0.765) and hexamer (0.765). It was observed that some C atoms were positive and some were negative. It was observed that the Mulliken atomic charges of the monomer, trimer and hexamer did not change in chain growth and remained close to each other.

Table 4. Dipole moments (D), polarizability (a.u.), and β components (esu) value of monomer, trimer and hexamer with the B3LYP method with 6-311G basis set.

Parameters	Monomer	Trimer	Hexamer	Parameters	Monomer	Trimer	Hexamer
μ_x	0.6121	−0.8235	−0.9571	β_{XXX}	65.078	44.258	−77.597
μ_y	0.5200	−0.7570	−1.3176	β_{XXY}	−64.772	−80.501	−150.95
μ_z	0.4329	−1.6520	−1.3128	β_{XYY}	−27.861	−106.20	196.99
$\mu_{(D)}$	0.9124	1.9951	2.0918	β_{YYY}	−23.820	−38.456	−3.6706
α_{xx}	−152.30	−256.25	−393.84	β_{XXZ}	84.171	−32.362	−144.24
α_{yy}	−166.10	−251.04	−373.96	β_{XYZ}	−8.1610	−75.937	42.042
α_{zz}	−168.345	−254.81	−405.50	β_{YYZ}	28.928	−51.803	−11.121
α_{XY}	2.3596	−17.230	−1.9930	β_{XZZ}	54.146	−35.006	−36.774
α_{XZ}	25.400	−12.212	30.755	β_{YZZ}	30.569	−0.7551	10.124
α_{YZ}	−2.4032	11.949	12.557	β_{ZZZ}	−10.647	16.751	−12.700
α(a.u.)	162.25	254.03	391.10	β (esu)	1.5×10^{-30}	1.7×10^{-29}	2.3×10^{-29}

3.3d *Molecular electrostatic potential:* As shown in figure 11, the molecular electrostatic potential (MEP) map with the B3LPY/6-311G (d,p) basis set was posed. The MEP shows that the region characterized by blue colour around the central atom has a positive charge [64,65]. In addition, the hydrogen atom in the ligands carries the maximum strength of the positive charge by dark blue colour. Most of the aromatic ring regions are almost neutral characterized by green colour. This was the same in three molecules.

The nonlinear optics (NLO) parameters of the monomer, trimer and hexamer for the gas phase compound were found as $\mu_{(D)}$ = 0.9124, 1.9951 and 2.0918, α(a.u.) = –162.25, –254.03 and –391.10, β (esu) = 1.5×10^{-31}, 1.7×10^{-31} and 2.3×10^{-31} respectively. This indicates that they can accept as NLO materials for monomer, trimer and hexamer (table 4). The increase in the number of monomers in the polymer chain caused the monitored parameters to change.

4. Conclusion

In this study, the RAFT polymerization, which has a unique position among controlled radical polymerizations, was investigated. The RAFT agents have an important contribution to controlled radical polymerization in the construction of molecular architecture. An influential polymerization with the RAFT agents has been achieved in the polymerization of styrene monomer. It appeared that the experimental consequences are equivalent to the calculation consequences. In addition, DFT/B3LYP method with 6-311G (d,p) basis set was preferred to analyse polymeric RAFT agent. With the above considerations in mind, the choice of different oligomers can facilitate information about polymer structure. The energy difference between HOMO and LUMO orbitals is 4.0 eV. This energy gap clearly explains the charge transfer of interaction within molecules. After optimization the bond lengths, angles the polarizability and the dipole moment were found. All electronic properties of oligomers are optically active and have NLO properties. Electrostatic potential surface and electron density isosurface mapping were used to explain the size, shape, charge density distribution, and chemical reactivity of oligomers.

References

[1] Fang J, Gao X and Luo Y 2020 *Polymer* **201** 122602
[2] Zakharova N V, Simonova M A, Zelinskii S N, Annenkov V V and Filippov A P 2019 *J. Mol. Liq.* **292** 111355
[3] Williams B M, Barone V, Pate B D and Peralta J E 2015 *Comput. Mater. Sci.* **96** 69
[4] Ishitsuka K, Pagaduan J N M, Kamon Y and Hashidzume A 2020 *Mater. Today Commun.* **22** 100689
[5] Tian J and Zhang W 2019 *Prog. Polym. Sci.* **95** 65
[6] Uyar Z, Turgut F, Arslan U, Durgun M and Degirmenci M 2019 *Eur. Polym. J.* **119** 102
[7] Abousalman-Rezvani Z, Eskandari P, Roghani-Mamaqani H and Salami-Kalajahi M 2020 *Adv. Colloid Interface Sci.* **278** 102126
[8] Eskandari P, Abousalman-Rezvani Z, Roghani-Mamaqani H, Salami-Kalajahi M and Mardani H 2019 *Adv. Colloid Interface Sci.* **273** 102021
[9] Qiao X G, Zhou Z, Pang X C, Lansalot M and Bourgeat-Lami E 2019 *Polymer* **172** 330
[10] Simula A, Ballard N, Aguirre M, Leiza J R, Es S V and Asua J M 2019 *Eur. Polym. J.* **110** 319
[11] Wang Y, Clay A and Nguyen M 2020 *Polymer* **188** 122097
[12] Zhang Z, Wang X, Tam K C and Sèbe G 2019 *Carbohydr. Polym.* **205** 322
[13] Kartal B, Yildiko U, Ozturk S, Ata A C and Cakmak I 2014 *J. Macromol. Sci. A* **51** 990
[14] Ponnupandian S, Chakrabarty A, Mondal P, Hoogenboom R, Lowe A B and Singha N K 2020 *Eur. Polym. J.* **131** 109679
[15] Cuervo-Rodriguez R, Bordegé V, Fernández-Monreal M C, Fernández-García M and Madruga E L 2004 *J. Polym. Sci. A Polym. Chem.* **42** 4168
[16] Allen M H, Hemp S T, Zhang M, Zhang M, Smith A E, Moore R B and Long T E 2013 *Polym. Chem.* **4** 2333

[17] Bussels R, Bergman-Göttgens C, Meuldijk J and Koning C 2005 *Polymer* **46** 8546
[18] Perrier S and Takolpuckdee P 2005 *J. Polym. Sci. A Polym. Chem.* **43** 5347
[19] Foster J C, Radzinski S C, Lewis S E, Slutzker M B and Matson J B 2015 *Polymer* **79** 205
[20] Vázquez-Dorbatt V, Tolstyka Z P and Maynard H D 2009 *Macromolecules* **42** 7650
[21] Bulmus V 2011 *Polym. Chem.* **2** 1463
[22] De P, Li M, Gondi S R and Sumerlin B S 2008 *J. Am. Chem. Soc.* **130** 11288
[23] Sumerlin B S 2012 *ACS Macro Lett.* **1** 141
[24] Ratcliffe L P D, Ryan A J and Armes S P 2013 *Macromolecules* **46** 769
[25] Warren N J and Armes S P 2014 *J. Am. Chem. Soc.* **136** 10174
[26] Figg C A, Simula A, Gebre K A, Tucker B S, Haddleton D M and Sumerlin B S 2015 *Chem. Sci.* **6** 1230
[27] Kang Y, Pitto-Barry A, Maitland A and O'Reilly R K 2015 *Polym. Chem.* **6** 4984
[28] Vana P, Davis T and Barner-Kowollik C 2002 *Macromol. Theory Simul.* **11** 823
[29] Wang A R and Zhu S 2003 *J. Polym. Sci. A Polym. Chem.* **41** 1553
[30] Deepak Sharma S, Kumar A, Kumar R, Nandy K, Srivastava A, Tomar M S *et al* 2019 *Mater. Today Commun.* **18** 14
[31] Mori H and Endo T 2012 *Macromol. Rapid Commun.* **33** 1090
[32] Liu Q, Wu H, Zhang L, Zhou Y, Zhang W, Pan X *et al* 2016 *Polym. Chem.* **7** 2015
[33] Akman M, Ata A Ç, Yildiko Ü and Cakmak İ 2020 *Int. J. Chem. Technol.* **4** 49
[34] Liu Y and Liu H 2018 *AIChE J.* **64** 238
[35] Stace S, Moad G, Fellows C and Keddie D 2015 *Polym. Chem.* **6** 7119
[36] Göktaş M 2019 *JIST* **9** 139
[37] Couture G and Ameduri B 2012 *Eur. Polym. J.* **48** 1348
[38] York A W, Kirkland S E and McCormick C L 2008 *Adv. Drug Deliv. Rev.* **60** 1018
[39] Bernard J, Favier A, Davis T P, Barner-Kowollik C and Stenzel M H 2006 *Polymer* **47** 1073
[40] Yeh K M and Chen Y 2008 *Synth. Met.* **158** 411
[41] Sandeau A, Mazières S and Destarac M 2012 *Polymer* **53** 5601
[42] Mun H, Hwang K and Kim W 2019 *J. Appl. Polym. Sci.* **136** 47069
[43] Guzmán H, Farkhondehfal M A, Tolod K R, Hernández S and Russo N 2019 F Calise, M D D'Accadia, M Santarelli, A Lanzini, D Ferrero (eds) In *Solar hydrogen production* (Academic Press) p 365
[44] Laursen S and Poudyal S 2015 F Shi and B Morreale (eds) In *Novel materials for carbon dioxide mitigation technology* (Amsterdam: Elsevier) p 233
[45] Pederson M R and Baruah T 2015 E Arimondo, C C Lin, S F Yelin (eds) In *Advances in atomic, molecular, and optical physics* (Amsterdam: Elsevier) p 153
[46] Munakata T 1990 (ed) In *Strongly coupled plasma physics* (North Holland, American Meteorological Society) p 695
[47] Afzal M A F and Hachmann J 2019 *Phys. Chem. Chem. Phys.* **21** 4452
[48] Frisch M J, Trucks G W, Schlegel H B, Scuseria G E, Robb M A, Cheeseman J R *et al* 2016 Wallingford CT. https://gaussian.com
[49] Latelli N, Ouddai N, Arotçaréna M, Chaumont P, Mignon P and Chermette H 2014 *Comput. Theor. Chem.* **1027** 39
[50] Gunasekar K, Chakravarthi N, Cho W, Lee J W, Kim S W, Cha S-H *et al* 2015 *Synth. Met.* **205** 185
[51] Priya M K, Revathi B K, Renuka V, Sathya S and Asirvatham P S 2019 *Mater. Today Proceed.* **8** 37
[52] Alcolea Palafox M, Bhat D, Goyal Y, Ahmad S, Hubert Joe I and Rastogi V K 2015 *Spectrochim. Acta A Mol. Biomol. Spectrosc.* **136 B** 464
[53] Prabhaharan M, Prabakaran A R, Gunasekaran S and Srinivasan S 2015 *Spectrochim. Acta A Mol. Biomol. Spectrosc.* **136** 494
[54] El Bourakadi K, Mekhzoum M E M, Boeré R T, Qaiss A E K and Bouhfid R 2020 *J. Mol. Struct.* **1202** 127253
[55] Demir P and Akman F 2017 *J. Mol. Struct.* **1134** 404
[56] Srivastava A K, Pandey A K, Jain S and Misra N 2015 *Spectrochim. Acta A Mol. Biomol. Spectrosc.* **136 B** 682
[57] Khajehzadeh M and Moghadam M 2017 *Spectrochim. Acta A Mol. Biomol. Spectrosc.* **180** 51
[58] Zeghbroeck B V 2011 *Principles of semiconductor devices* (Colorado Press, USA) Chapter 2. https://ecee.colorado.edu/~bart/book/book/content2
[59] Yang Y J, Kan Y H, Su Z M and Zhao L 2005 *J. Mol. Struct.: Theochem.* **725** 127
[60] Sworakowski J 2018 *Synth. Met.* **235** 125
[61] Anand S, Sundararajan R S, Ramachandraraja C, Ramalingam S and Durga R 2015 *Spectrochim. Acta A Mol. Biomol. Spectrosc.* **138** 203
[62] Abkari A, Chaabane I and Guidara K 2016 *Physica E Low Dimens. Syst. Nanostruct.* **81** 136
[63] Komjáti B, Urai Á, Hosztafi S, Kökösi J, Kováts B, Nagy J *et al* 2016 *Spectrochim. Acta A Mol. Biomol. Spectrosc.* **155** 95
[64] Demircioğlu Z, Kaştaş G, Kaştaş Ç A and Frank R 2019 *J. Mol. Struct.* **1191** 129
[65] Gelfand N, Freidzon A and Vovna V 2019 *Spectrochim. Acta A Mol. Biomol. Spectrosc.* **216** 161